AJNR

Diffusion Tensor Imaging Shows Different Topographic Involvement of the Thalamus in Progressive Supranuclear Palsy and Corticobasal Degeneration

A. Erbetta, M.L. Mandelli, M. Savoiardo, M. Grisoli, A. Bizzi, P. Soliveri, L. Chiapparini, S. Prioni, M.G. Bruzzone and F. Girotti

ORIGINAL
RESEARCH

A. Erbetta
M.L. Mandelli
M. Savoiardo
M. Grisoli
A. Bizzi
P. Soliveri
L. Chiapparini
S. Prioni
M.G. Bruzzone
F. Girotti

Diffusion Tensor Imaging Shows Different Topographic Involvement of the Thalamus in Progressive Supranuclear Palsy and Corticobasal Degeneration

BACKGROUND AND PURPOSE: In progressive supranuclear palsy (PSP) and corticobasal degeneration (CBD), postmortem studies show different topographic involvement of the thalamus, basal ganglia, and their cortical connections. Diffusion tensor imaging (DTI) is an MR imaging technique sensitive to gray and white matter microstructure integrity. This study was performed to determine whether DTI may demonstrate microstructural differences between PSP and CBD, particularly within the thalamus and its cortical connections.

MATERIALS AND METHODS: Nine patients with probable PSP, 11 with probable CBD, and 7 controls formed the study group. Apparent diffusion coefficient average (ADC_{ave}) and fractional anisotropy (FA) values were measured in regions of interest positioned in the ventrolateral (motor), medial, anterior, and posterior regions of the thalami, basal ganglia, fronto-orbital white matter, cingulum, supplementary motor area (SMA), and precentral and postcentral gyri in patients and controls.

RESULTS: In PSP, ADC_{ave} values were increased in several areas: the thalamus, particularly in its anterior and medial nuclei; cingulum; motor area; and SMA. FA values were particularly decreased in the fronto-orbital white matter, anterior cingulum, and motor area. In CBD, ADC_{ave} was increased in the motor thalamus, in the precentral and postcentral gyri, ipsilateral to the affected frontoparietal cortex, and in the bilateral SMA. FA was mainly decreased in the precentral gyrus and SMA, followed by the postcentral gyrus and cingulum.

CONCLUSIONS: In patients with PSP, thalamic involvement was diffuse and prevalent in its anterior part, whereas in CBD involvement was asymmetric and confined to the motor thalamus. DTI may be useful in the differential diagnosis of these 2 parkinsonian disorders.

Progressive supranuclear palsy (PSP) and corticobasal degeneration (CBD) are pathologically distinct causes of progressive atypical parkinsonism poorly or not responsive to levodopa. Both disorders are characterized by τ protein (4R isoform) deposits in neurons and glia.[1] However, the brain areas involved in the 2 conditions differ,[2] mainly the cortex in CBD and the subcortical areas in PSP.[3] Although diagnostic criteria are based on motor impairment, the clinical hallmarks of these conditions,[4,5] in both disorders cognitive decline and behavioral abnormalities are always present and dementia is frequent.[6,7]

In PSP, anterior frontal lobe dysfunction is the most disabling cognitive deficit, partly due to marked deafferentation of the prefrontal areas, resulting from degeneration of striato-thalamocortical pathways.[8,9] The circuits implicated in behavioral control involve the thalamus, mainly the medial thalamus connected to the fronto-orbital cortex and the anterior thalamus connected to the cingulate gyrus.[10]

In CBD, cognitive and motor dysfunctions are frequent, and the most characteristic higher cortical disorders are limb-kinetic apraxia, ideomotor apraxia, and alien limb phenomenon, probably related to damage to the perirolandic regions.[11] These cortical areas are functionally connected to the motor thalamus, a group of nuclei in the lateral part of the thalamus.

Conventional MR imaging in PSP shows midbrain atrophy, particularly the dorsal midbrain; signal intensity changes in the tegmentum and periaqueductal gray matter,[12] and marked enlargement of the third ventricle, suggesting thalamic tissue loss.[13] Recent studies with voxel-based morphometry (VBM) have confirmed thalamic atrophy and additionally report symmetric tissue loss in the orbitofrontal cortex and anterior cingulate cortex.[14,15]

Conventional MR imaging in CBD shows asymmetric cortical atrophy in the frontoparietal regions, which is worse contralateral to the clinically affected side; basal ganglia and thalamic involvement is rarely visible.[7]

Diffusion tensor imaging (DTI) measures the translational movement of water molecules in biologic tissues. It measures fractional anisotropy (FA), an index of white matter coherence and axonal packing, and apparent diffusion coefficient average (ADC_{ave}), an index of the average magnitude of the rate of diffusion within each voxel. A reduction in the linear organization of white matter pathways will determine a decrease in FA. White and gray matter damage, even at the microstructural level, will determine an increase in ADC_{ave}.

Postmortem pathologic studies have shown loss of neurons, with τ protein aggregates in the thalamus of both tauopathies; however, the topographic distribution of lesions differs between PSP and CBD.[2]

The aim of this study was to determine whether, in these diseases, DTI can detect a different distribution of microstructural tissue damage occurring in the thalamus, the basal ganglia, and their connections with cortical areas. Thus DTI metrics in the thalami could be used in the differential diagnosis of the 2 parkinsonian disorders.

Materials and Methods

Nine patients with PSP (5 women, 4 men; mean age, 66.5 years; range, 51–73 years), 11 patients with CBD (7 women and 4 men; mean age, 66.4 years; range, 51–77 years), and 7 healthy volunteer controls of an age as similar as possible to that of the patients (2 women and 5 men; mean age, 60.4 years; range, 55–66 years) were enrolled in this study. The controls had no history or signs of neurologic disease or cognitive disturbance and had normal brain MR imaging findings. For the MR imaging examinations, written informed consent was obtained from all participants.

Patients were diagnosed according to accepted clinical criteria[4,5] and displayed typical features of the diseases. The Unified Parkinson's Disease Rating Scale (UPDRS III) was used to assess motor disability; the Mini-Mental State Examination (MMSE), to assess mental state. In patients with CBD, akinetic rigid syndrome and limb apraxia were more marked on the side contralateral to MR imaging−detected hemispheric atrophy and signal-intensity abnormalities (6 clinically worse on the right side, 5 on the left).

Imaging

A 1.5T MR imaging system (Avanto; Siemens, Erlangen, Germany) was used. Axial proton attenuation/T2-weighted images (TR = 3500 ms; TE = 17 and 84 ms; 5-mm thickness), coronal turbo spin-echo T2-weighted images (TR = 4100 ms, TE = 143 ms, 5-mm thickness), and axial gradient-echo T2*-weighted images (TR = 700 ms, TE = 26 ms, 5-mm thickness) were obtained. Volumetric T1-weighted images were acquired by using a magnetization-prepared rapid acquisition of gradient echo sequence (160 sagittal sections, TR = 1640 ms, TE = 2.0 ms, TI = 552 ms, voxel size = 1 mm^3, flip angle = 12°).

DTI was performed by using twice-refocused single-shot spin-echo echo-planar sequences in axial sections with the following settings: TR = 7500 ms, TE = 80 ms, NEX = 10, matrix = 192 × 256, FOV = 180 × 240 mm, section thickness = 2.5 mm, and no intersection gap. DTI was performed along 12 directions with a b=1000 s/mm^2. In addition, images without diffusion weighting were acquired corresponding to b=0 s/mm^2. Diffusion-weighted images were corrected for eddy current and then corrected for head motion by using the Linear Image Registration Tool software of the Centre for Functional Magnetic Resonance Imaging of the Brain (University of Oxford, Oxford, UK) with 12 df. The acquisitions were repeated 5 times to improve the signal intensity–to-noise ratio and subsequently averaged.

The conventional images were assessed jointly by 2 senior neuroradiologists (A.E., M.G.) for supratentorial and infratentorial atrophy and signal-intensity changes. Particular attention was paid to the presence/absence of bilateral/unilateral frontoparietal atrophy, ipsilateral ventricular dilation, third ventricle enlargement, cortical or subcortical signal-intensity abnormalities, basal ganglia atrophy, midbrain atrophy (with anteroposterior diameter measurement), and tegmental signal-intensity abnormalities. MR images of controls were assessed similarly.

Image Analysis

The tensor was estimated statistically by using a multivariate linear regression model assuming a monoexponential relationship between signal intensity and the product of the b matrix and diffusion tensor matrix components.[16] ADC$_{ave}$ and FA maps were calculated by using DTIStudio software[17] (Johns Hopkins University, Baltimore, Md) and were measured within several regions of interest. Circular regions of interest were identified independently by the same 2 neuroradiologists on DTI color maps and on DTI echo-planar images with b=0 s/mm^2. The regions of interest were transferred to ADC$_{ave}$ and FA maps. To minimize partial volume effects, we chose 2- to 4-mm-diameter regions of interest. In the deep gray nuclei, regions of interest were positioned bilaterally in the head of the caudate nucleus; in the central part of the globus pallidus and putamen; and in the anterior, medial, lateral (motor), and posterior thalamus, identified according to the *Stereotactic Atlas of the Human Thalamus and Basal Ganglia* by Anne Morel.[18,19] More specifically, the region of interest placed in the anterior thalamus was positioned in the forward part of the nucleus close to the genu of the internal capsule, posterolateral to the anterior column of the fornix. The regions of interest in the medial and the motor thalamus were positioned in the same coronal plane of the corticospinal tract in the posterior limb of the internal capsule, close to the third ventricle and to the posterior limb of the internal capsule, respectively. The region of interest in the posterior thalamus was positioned 8–10 mm posterolateral to the motor thalamus.

White matter regions of interest were positioned in the superior cerebellar peduncle, lateral prefrontal and fronto-orbital regions, cingulum, white matter in proximity to the supplementary motor area (SMA), and white matter of the precentral (hand knob region) and postcentral gyri at the same distance off the midline. The following are more detailed positions: 1) In the prefrontal lateral region, regions of interest were located in the white matter of the frontal operculum in the inferior frontal gyrus; 2) in the fronto-orbital region, regions of interest were positioned in the white matter of the medial supraorbital gyrus; 3) the cingulum was evaluated in its anterior segment (in front of the genu of the corpus callosum) and posterior segment (behind the splenium), where the bundles run caudocranially and appear blue on the color map; 4) the SMA was identified as the parasagittal gyrus bounded posteriorly by the primary motor cortex and anteriorly by a coronal plane containing the vertical line intersecting the anterior commissure and perpendicular to the anteroposterior commissure plane.[20] ADC values were measured in all the regions of interest, both in white matter and gray matter areas. FA measurements were obtained in the white matter and in the thalami because of their high content of white matter fibers. All region-of-interest positions are illustrated in Figs 1 and 2.

Statistical Analysis

The difference in sex distribution between groups was evaluated by the χ^2 test. Age differences were investigated by 1-way analysis of variance (ANOVA) followed by the Tukey correction. Differences in disease duration and UPDRS and MMSE scores were assessed by the nonparametric Mann-Whitney U test because of the small sample size. The inter-rater and intrarater reliability of ADC$_{ave}$ and FA measurements was determined by intraclass correlation coefficients derived by using a 1-way random-effects ANOVA model. The inter-rater reliability was estimated on all scans. The intrarater reliability was estimated on 10 scans evaluated by the first rater. The values were then averaged, and the mean was used.

After confirming the absence of lateralization of ADC$_{ave}$ and FA
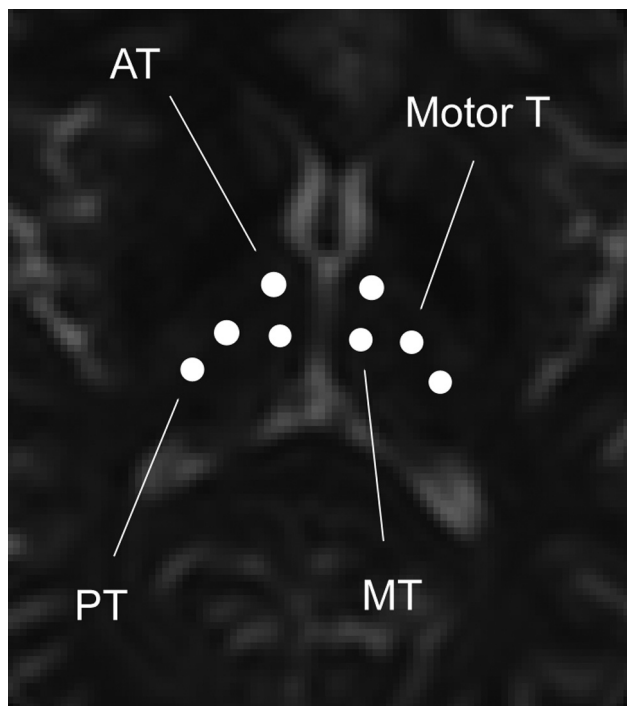
Fig 1. Positioning of regions of interest for ADC and FA measurement in the thalami. AT indicates anterior thalamus; motor T, motor thalamus; MT, medial thalamus; PT, posterior thalamus.

changes in patients with PSP and controls by a paired t test, we averaged measurements from the 2 hemispheres. For patients with CBD, measurements from each side were averaged for regions for which no differences between the 2 sides were found; otherwise the value of the most affected side (ie, the higher ADC_{ave} and the lower FA value) was used.

One-way ANOVA with group as a factor, followed by the Tukey test for multiple comparisons, was used to assess differences in ADC_{ave} and FA measurements among the 3 groups after determining that the distributions of values were normal by the Shapiro-Wilk normality test. Differences were considered significant for $P < .05$. Results are reported as means and SDs. The analyses were performed with the Statistical Package for the Social Sciences, Version 13.0 for Windows (SPSS, Chicago, Ill).

Results
Demographics and clinical data of patients and controls are reported in On-line Table 1. The ANOVA did not show any significant difference in age between groups. The inter-rater and intrarater reliability analysis showed good agreement ($r >$ 0.85, $r > 0.83$, respectively). The results of the statistical analyses of the selected brain regions for ADC_{ave} are reported in On-line Table 2 and for FA, in On-line Table 3.

Apparent Diffusion Coefficients
ANOVA showed significant differences among groups for ADC_{ave} in the caudate nucleus (F = 5.343, $P = .012$), globus pallidus (F = 3.952, $P = .033$), anterior (F = 7.433, $P = .003$), medial (F = 4.360, $P = .024$) and motor thalami (F = 7.713, $P = .003$), superior cerebellar peduncle (F = 4.503, $P = .022$), anterior (F = 3.542, $P = .045$) and posterior cingula (F = 4.085, $P = .030$), SMA (F = 7.416, $P = .003$), and precentral

(F = 20.37, $P < .001$) and postcentral gyri (F = 12.51, $P < .001$).

In patients with PSP compared with controls, the Tukey test showed an ADC_{ave} increase in the head of the caudate nucleus ($P = .015$), globus pallidus ($P = .026$), anterior thalamus ($P = .004$), and medial ($P = .049$) and motor thalami ($P = .015$). The ADC_{ave} was also increased in the superior cerebellar peduncle ($P = .04$), anterior cingulum ($P = .043$), and posterior cingulum ($P = .027$), SMA ($P = .045$), and the precentral gyrus ($P = .027$).

In patients with CBD compared with controls, we found increased ADC_{ave} in the head of the caudate nucleus ($P = .028$), motor thalamus ($P = .002$), SMA ($P = .002$), precentral gyrus ($P < .001$), and postcentral gyrus ($P < .001$).

In the comparison between patients with PSP and CBD, we found higher ADC_{ave} values in patients with PSP in the anterior thalamus ($P = .018$), medial thalamus ($P = .041$), and the superior cerebellar peduncle ($P = .042$). Higher ADC_{ave} values were found in patients with CBD in the precentral ($P = .004$) and postcentral gyri ($P = .021$).

Fractional Anisotropy
ANOVA showed significant differences between groups for FA in the fronto-orbital area (F = 5.764, $P = .009$), anterior (F = 14.85, $P < .001$) and posterior (F = 5.263, $P = .013$) cingula, SMA (F = 7.19, $P = .004$), precentral gyrus (F = 29.032, $P < .001$), and postcentral gyrus (F = 4.760, $P = .018$). In patients with PSP compared with controls, the Tukey test showed that FA was lower in the fronto-orbital area ($P = .007$), anterior cingulum ($P < .001$), posterior cingulum ($P = .012$), SMA ($P = .031$), precentral gyrus ($P < .001$), and postcentral gyrus ($P = .031$). In patients with CBD compared with controls, we found that FA was lower in the anterior cingulum ($P = .028$), posterior cingulum ($P = .047$), SMA ($P = .003$), precentral gyrus ($P < .001$), and postcentral gyrus ($P = .027$). In the comparison between patients with PSP and CBD, we found that FA was lower in the anterior cingulum ($P = .013$) in patients with PSP.

Discussion
The most important finding of this study was that DTI metrics (ADC_{ave}) are sensitive enough to detect lesion topography differences in the thalamus between patients with PSP and CBD. The anterior and medial thalamic nuclei were involved only in patients with PSP. The motor thalamus was involved in both tauopathies, but abnormalities were asymmetric in CBD and symmetric in PSP.

Significant differences in ADC_{ave} and FA abnormalities were found also in other brain regions. The anterior cingulum—functionally connected to the anterior thalamus—was characterized by high ADC_{ave} and low FA in patients with PSP. The fronto-orbital region—functionally connected to the medial thalamus—was characterized by abnormally low FA in patients with PSP. Abnormal ADC_{ave} and FA values were measured in the primary motor cortex and SMA, which are functionally connected to the motor thalamus in both tauopathies. In the postcentral gyrus, FA was abnormal in both, whereas ADC_{ave} was increased only in patients with CBD. This study shows that DTI detects microstructural changes in vulnerable gray and white matter regions of patients with tauopathies,
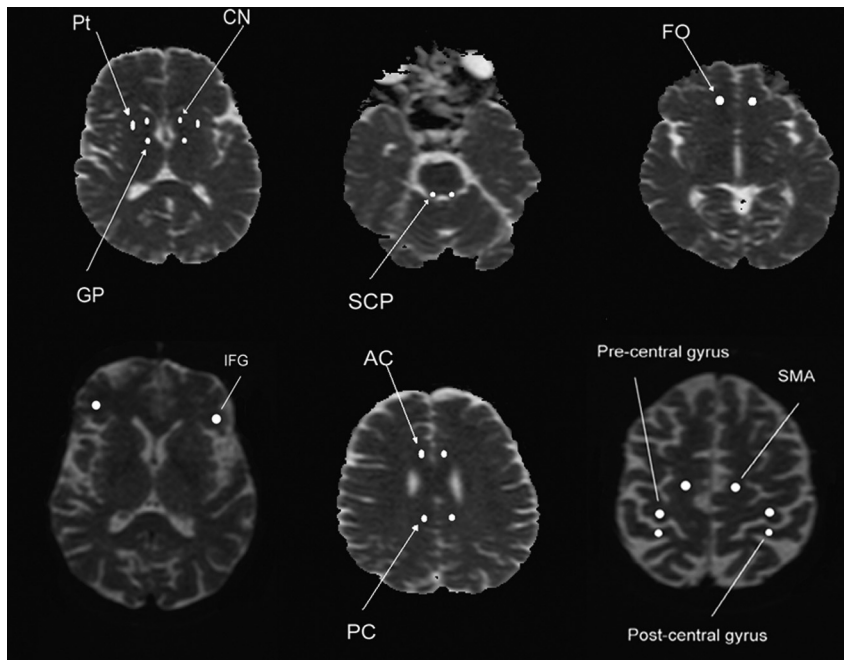
Fig 2. Positioning of regions of interest for ADC and FA measurement in the basal ganglia and white matter. CN indicates caudate nucleus; GP, globus pallidus; Pt, putamen; SCP, superior cerebellar peduncle; FO, fronto-orbital gyrus; IFG, inferior frontal gyrus; AC, anterior cingulum; PC, posterior cingulum; SMA, supplementary motor area.

despite the absence of signal-intensity abnormalities on conventional MR imaging. Peculiar to this study was the demonstration that significant FA and ADC_{ave} abnormalities are found in anatomic brain regions that are known a priori to be functionally connected.

This study implies that pathologic changes such as the formation of τ protein aggregates and neuronal loss in the gray matter of patients with PSP and CBD result in elevation of the ADC_{ave}, probably due to diminished tissue organization, which represents microstructural barriers to diffusion of water in the interstitium. Decreased FA in white matter connecting affected gray matter regions may imply that loss of coherence, reduction of axonal packing, and demyelination have occurred, probably secondary to wallerian degeneration. In neurodegenerative diseases, decreasing FA has often been associated with elevation of ADC_{ave}, even though the 2 metrics measure different physical phenomena. Although in neurodegenerative diseases the ADC_{ave} is essentially related to the structure of the tissue and the amplitude of the extracellular spaces that limit the movements of the water molecules (and is therefore suitable to study both gray and white matter), FA depends on the limitation of the water motion in a certain direction because it occurs in anisotropic tissue, in which the white matter fibers have a prevalent orientation.

This study was the first to investigate regional analysis in the thalamus with DTI parameters. Two previous studies[21,22] also demonstrated abnormally increased ADC_{ave} in the thalamus in comparison with that in healthy subjects but with a single large region of interest. Padovani et al[21] found abnormally decreased FA in the bilateral posterior thalamic radiations and anterior thalamus.

In the 1990s, few detailed neuropathologic studies had examined the topographic distribution and density of neurofibrillary tangles in the thalamus of patients with PSP.[23-25] Subsequently, the presence of large numbers of intracellular neurofibrillary tangles was demonstrated in the medial thalamus of patients with PSP, with similar but less pervasive involvement of the anterior thalamus.[26] The anterior thalamic nuclei are connected to the cingulate gyrus, and the medial thalamic nuclei are connected to the fronto-orbital gyrus. These connections are part of the limbic circuits involved in behavioral control.[10] Abnormalities in these circuits in patients with PSP may explain the apathy, reduced verbal fluency, and motor inhibition. Our findings of abnormal ADC_{ave} or FA values in the anterior and medial thalami and anterior cingulate gyrus and fronto-orbital regions are also consistent with morphometric abnormalities identified by VBM.[14] Furthermore, they correlate well with the functional-anatomic models of the behavioral disturbances that characterize PSP.[7]

In accordance with Seppi et al,[27] abnormally high ADC_{ave} in the head of the caudate nucleus was documented. The head of the caudate is connected to dorsolateral prefrontal areas and is a component of the striatothalamocortical circuits involved in executive functions, which are also compromised in PSP. We found, however, that ADC_{ave} and FA were normal in the inferior frontal gyrus, part of the dorsolateral prefrontal area, possibly due to the small size of the regions of interest compared with the region under analysis.

The globus pallidus is severely affected in PSP, mainly in its external part.[28] Together with the ventrolateral and ventroanterior nuclei of the thalamus (motor thalamus), the globus pallidus participates in the motor circuit linking the basal ganglia to the motor cortex, premotor cortex, and SMA.[28-31] Our findings, of abnormally high ADC_{ave} in the globus pallidus and lateral part of the thalamus, together with low FA in the primary motor cortex and SMA, are consistent with postmortem studies.[32] Our findings in the primary motor area are also consistent with the results of other imaging studies.[21,22,27,33] These abnormalities in multiple areas of the mo-

tor circuit may help explain motor dysfunctions such as kinetic apraxia, frequently observed in patients with PSP.[34]

ADC$_{ave}$ abnormalities were not found in the putamen, despite its involvement in PSP. The anatomic architecture of the putamen and its connections are complex, and multiple region-of-interest analysis, such as that performed in the thalamus, may be necessary to identify selected topographic abnormalities.

As expected, we found abnormally high ADC$_{ave}$ in the superior cerebellar peduncle only in patients with PSP, in line with imaging and postmortem studies showing atrophy.[35] However, FA was not abnormal in this structure, suggesting that coherence and packaging of the bundles were preserved.

In this study, in CBD, abnormally elevated ADC$_{ave}$ in the motor thalamus, precentral and postcentral gyri of the atrophic hemisphere and bilaterally in the caudate and SMA was shown. Abnormally low FA in the primary motor area, SMA, postcentral gyrus, and anterior and posterior cingulate gyri were shown. These findings are consistent with those in postmortem studies. Gross examination of the brain usually shows asymmetric atrophy of gyri most marked in pre- and postcentral regions, where swollen and vacuolated cortical neurons (ballooned neurons) and neurofibrillary tangles are found.[36,37] Neuronal loss, gliosis, and neurofibrillary tangles also characterize lesions in the motor thalamus.[38] Conventional MR imaging demonstrates asymmetric pericentral cortical atrophy in most cases, and hyperintensity of the atrophic cortex and underlying white matter may be seen on fluid-attenuated inversion recovery images.[39] VBM studies have confirmed that cortical atrophy in the pericentral regions is clearly asymmetric in CBD and, in this respect, differs from that in PSP.[40]

Although conventional MR imaging investigations do not reveal thalamic involvement in CBD, fluorodeoxyglucose–positron-emission tomography and hexamethylpropylene-amine oxime−single-photon emission CT have shown asymmetric hypometabolism in the thalamus, precentral and postcentral gyri, and striatum.[41] Our data delineate thalamic involvement in CBD in greater spatial detail, demonstrating abnormally high ADC$_{ave}$ in the motor thalamus contralateral to the clinically affected side. We also found increased ADC$_{ave}$ in the head of the caudate nucleus, but not in the putamen or in the globus pallidus. In view of abnormal ADC$_{ave}$ and FA in the postcentral gyrus, we noted that ADC$_{ave}$ was normal in the functionally connected ipsilateral posterior thalamus.

The distribution of the abnormalities observed in our patients with CBD is consistent with the clinical presentation characterized by cortical sensory disturbances, motor clumsiness, and limb-kinetic apraxia. Our results are also consistent with a DTI study[42] in CBD that showed decreased FA in dorsolateral frontoparietal association tracts and in intraparietal (arcuate) bundles, despite substantial methodologic differences in data analysis. This study did not specifically evaluate DTI parameters in subregions of the thalamus, except for the pulvinar. A more recent diffusion study that evaluated only ADC$_{ave}$ values demonstrated that hemispheric asymmetry was able to discriminate patients with CBD from those with PSP and Parkinson disease. However differences in the thalami did not reach statistical significance.[43]

Limitations

There are a few limitations in this study. Confirmation of clinical diagnoses with postmortem examinations was not available. The number of patients was small as expected in relatively rare diseases. Some of the regions that we evaluated, such as the inferior frontal gyrus, have significant crossing fibers. In future studies, more optimized DTI methodologies such as diffusion spectrum imaging may help to solve this problem.[44] The use of greater magnet field strength (3T) and a greater than 12-direction protocol would also be of further advantage in future studies.

Conclusions

Despite these limitations, our study showed that DTI parameters are sensitive to selected tissue microscopic degeneration in distinct areas of the thalami and their white matter connections to the cortex. The spatial distribution of diffusivity alterations in the thalamus was different between patients with PSP and CBD. Thus DTI metrics may be useful in the differential diagnosis of these 2 parkinsonian disorders. However, evaluations of cognitive and behavioral disorders in a larger series of patients with PSP and CBD studied with DTI are necessary to establish more precise correlations between specific cognitive and motor dysfunctions and anatomic areas in which microstructural abnormalities are demonstrated.

References

1. Di Maria E, Tabaton M, Vigo T, et al. **Corticobasal degeneration shares a common genetic background with progressive supranuclear palsy.** *Ann Neurol* 2000;47:374–77
2. Hattori M, Hashizume Y, Yoshida M, et al. **Distribution of astrocytic plaques in the corticobasal degeneration brain and comparison with tuft-shaped astrocytes in the progressive supranuclear palsy brain.** *Acta Neuropathol* 2003;106:143–49. Epub 2003 May 2
3. Arvanitakis Z, Wszolek ZK. **Recent advances in the understanding of tau protein and movement disorders.** *Curr Opin Neurol* 2001;14:491–97
4. Litvan I, Agid Y, Calne D, et al. **Clinical research criteria for the diagnosis of progressive supranuclear palsy Steele-Richardson-Olszewski syndrome: report of the NINDS-SPSP international workshop.** *Neurology* 1996;47:1–9
5. Kumar R, Bergeron C, Pollanen MS, et al. **Cortical-basal ganglionic degeneration.** In: Jankovic J, Tolosa E, eds. *Parkinson's Disease and Movement Disorders.* 3rd ed. Baltimore: Williams & Wilkins Press; 1998:297–316
6. Maher ER, Lees AJ. **The clinical features and natural history of the Steele-Richardson-Olszewski syndrome progressive supranuclear palsy.** *Neurology* 1986;36:1005–08
7. Soliveri P, Monza D, Paridi D, et al. **Cognitive and magnetic resonance aspects of corticobasal degeneration and progressive supranuclear palsy.** *Neurology* 1999;53:502–07
8. Soliveri P, Monza D, Paridi D, et al. **Neuropsychology follow-up in patients with Parkinson's disease, striatonigral degeneration-type multisystem atrophy, and progressive supranuclear palsy.** *J Neurol Neurosurg Psychiatry* 2000;69:313–18
9. Litvan I, Phipps M, Pharr VL, et al. **Randomized placebo controlled trial of donepezil in patients with progressive supranuclear palsy.** *Neurology* 2001;57:467–73
10. Cummings JL. **Frontal-subcortical circuits in human behavior.** *Arch Neurol* 1993;50:873–80
11. Schneider JA, Watts RL, Gearing M, et al. **Corticobasal degeneration: neuropathological and clinical heterogeneity.** *Neurology* 1997;48:959–69
12. Savoiardo M, Strada L, Girotti F, et al. **MR imaging in progressive supranuclear palsy and Shy-Drager syndrome.** *J Comput Assist Tomogr* 1989;13:555–60
13. Savoiardo M, Girotti F, Strada L, et al. **Magnetic resonance imaging in progressive supranuclear palsy and in other parkinsonian disorders.** *J Neural Transm Suppl* 1994;42:93–110
14. Cordato NJ, Duggins AJ, Halliday GM, et al. **Clinical deficits correlate with regional cerebral atrophy in progressive supranuclear palsy.** *Brain* 2005;128:1259–66
15. Boxer AL, Geschwind MD, Belfor N, et al. **Patterns of brain atrophy that differentiate corticobasal degeneration syndrome from progressive supranuclear palsy.** *Arch Neurol* 2006;63:81–86

16. Basser PJ, Mattiello J, LeBihan D. **Estimation of the effective self-diffusion tensor from the NMR spin echo.** *J Magn Reson B* 1994;103:247–54
17. Jiang H, van Zijl PC, Kim J, et al. **DtiStudio: resource program for diffusion tensor computation and fiber bundle tracking.** *Comput Methods Programs Biomed* 2006;81:106–16. Epub 2006 Jan 18
18. Wiegell MR, Tuch DS, Larsson HB, et al. **Automatic segmentation of thalamic nuclei from diffusion tensor magnetic resonance imaging.** *Neuroimage* 2003;19:391–401
19. Niemann K, Mennicken VR, Jeanmonod D, et al. **The Morel stereotactic atlas of the human thalamus: atlas-to-MR registration of internally consistent canonical model.** *NeuroImage* 2000;12:601–16
20. Picard N, Strick PL. **Motor areas of the medial wall: a review of their location and functional activation.** *Cereb Cortex* 1996;6:342–53
21. Padovani A, Borroni B, Brambati SM, et al. **Diffusion tensor imaging and voxel based morphometry study in early progressive supranuclear palsy.** *J Neurol Neurosurg Psychiatry* 2006;77:457–63
22. Paviour DC, Price SL, Stevens JM, et al. **Quantitative MRI measurement of superior cerebellar peduncle in progressive supranuclear palsy.** *Neurology* 2005;64:675–79
23. Steele JC, Richardson JC, Olszewski J. **Progressive supranuclear palsy: a heterogeneous degeneration involving the brain stem, basal ganglia and cerebellum with vertical gaze and pseudobulbar palsy, nuchal dystonia and dementia.** *Arch Neurol* 1964;10:333–59
24. Lantos PL. **The neuropathology of progressive supranuclear palsy.** *J Neural Transm Suppl* 1994;42:137–52
25. Matsumoto R, Nakano I, Arai N, et al. **Progressive supranuclear palsy with asymmetric lesions in the thalamus and cerebellum, with special reference to the unilateral predominance of many torpedoes.** *Acta Neuropathol* 1996;92:640–44
26. Henderson JM, Carpenter K, Cartwright H, et al. **Loss of thalamic intralaminar nuclei in progressive supranuclear palsy and Parkinson's disease: clinical and therapeutic implications.** *Brain* 2000;123:1410–21
27. Seppi K, Schocke MF, Esterhammer R, et al. **Diffusion-weighted imaging discriminates progressive supranuclear palsy from PD, but not from the parkinson variant of multiple system atrophy.** *Neurology* 2003;60:922–27
28. Hardman CD, Halliday GM. **The external globus pallidus in patients with Parkinson's disease and progressive supranuclear palsy.** *Mov Disord* 1999;14:626–33
29. DeVito JL, Anderson ME. **An autoradiographics study of efferent connections of the globus pallidus in Macaca mulatta.** *Exp Brain Res* 1982;46:107–17
30. Strick PL. **Anatomical analysis of ventrolateral thalamic input to primate motor cortex.** *J Neurophysiol* 1976;39:1020–31
31. Schell GR, Strick PL. **The origin of thalamic inputs to the arcuate premotor and supplementary motor area.** *J Neurosci* 1984;4:539–60
32. Halliday GM, Macdonald V, Henderson JM. **A comparison of degeneration in motor thalamus and cortex between progressive supranuclear palsy and Parkinson's disease.** *Brain* 2005;128(pt 10):2272–80. Epub 2005 Jul 13
33. Nicoletti G, Lodi R, Condino F, et al. **Apparent diffusion coefficient measurements of the middle cerebellar peduncle differentiate the Parkinson variant of MSA from Parkinson's disease and progressive supranuclear palsy.** *Brain* 2006;129(pt 10):2679–87. Epub 2006 Jun 30
34. Soliveri P, Piacentini S, Girotti F. **Limb apraxia and cognitive impairment in progressive supranuclear palsy.** *Neurocase* 2005;11:263–67
35. Tsuboi Y, Slowinski J, Joseph KA, et al. **Atrophy of the superior cerebellar peduncle in progressive supranuclear palsy.** *Neurology* 2003;60:1766–69
36. Dickson DW, Bergeron C, Chin SS, et al. **Office of rare diseases neuropathologic criteria for corticobasal degeneration.** *J Neuropathol Exp Neurol* 2002;61:935–46
37. Rebeiz JJ, Kolodny EH, Richardson EP. **Corticodentatonigral degeneration with neuronal achromasia.** *Arch Neurol* 1968;18:20–33
38. Gibb WR, Luthert PJ, Marsden CD. **Corticobasal degeneration.** *Brain* 1989;112:1171–92
39. Savoiardo M, Grisoli M, Girotti F. **Magnetic resonance imaging in CBD, related atypical parkinsonian disorders, and dementia.** *Adv Neurol* 2000;82:197–208
40. Josephs KA, Whitwell JL, Dickson DW, et al. **Voxel-based morphometry in autopsy proven PSP and CBD.** *Neurobiol Aging* 2008;29:280–89
41. Brooks DJ. **Functional imaging studies in corticobasal degeneration.** *Adv Neurol* 2000;82:209–15
42. Borroni B, Garibotto V, Agosti C, et al. **White matter changes in corticobasal degeneration syndrome and correlation with limb apraxia.** *Arch Neurol* 2008;65:796–801
43. Rizzo G, Martinelli P, Manners D, et al. **Diffusion-weighted brain imaging study of patients with clinical diagnosis of corticobasal degeneration, progressive supranuclear palsy and Parkinson's disease.** *Brain* 2008;131:2690–700
44. Wedeen VJ, Wang RP, Schmahmann JD, et al. **Diffusion spectrum magnetic resonance imaging (DSI) tractography of crossing fibers.** *Neuroimage* 2008;41:1267–77